Chapter 3 Hydrostatic Fluid Distribution

Reading assignment:
CENG 571, Chapter 3 Rock Properties; Pore size distribution, Thomeer model of the capillary pressure curve, Fit of capillary pressure with lognormal distribution

CENG 571, Chapter 5 Multiphase Fluid Distribution; Capillarity, Nonwetting phase trapping, Hysteresis

We discussed in CENG 571 how the pore size distribution may be characterized measuring a mercury - air (vacuum) capillary pressure curve for a rock sample. In this chapter we will discuss how the capillary pressure curve determines the hydrostatic distribution of fluids in porous media. We will also see that capillary pressure can have a significant effect in dynamic displacement processes. Capillary pressure adds the second spatial derivative of saturation to the mass conservation equations. This changes the saturation equation from hyperbolic to parabolic in nature. The capillary pressure has greatest effect on dynamic processes where the saturation gradient is large, e.g. at shock fronts. Also since the order of the spatial differentials increased from one to two, the system is influenced by a second boundary condition, i.e. specified capillary pressure at the outflow boundary.

Shape of Capillary Pressure Curves

We earlier associated the shape of the capillary pressure curve with the pore size distribution. We can view the shape of the drainage capillary pressure curve as if it is due to two contributions: (1) nonwetting fluid entering a circular capillary of a radius, r, and (2) nonwetting fluid entering a crevice such that the fluid interface has a mean radius of curvature equal to r. If the porous medium consists of a bundle of identical circular capillaries with a radius R, then the capillary pressure curve would be a horizontal line as the saturation goes from 1.0 to zero at the common entry capillary pressure of all capillaries. If the porous medium is a bundle of capillary tubes with a distribution of radii, then the capillary pressure curve will be given by the cumulative size distribution. Suppose now that the porous media is made up of a bundle of uniform circular rods with a cubic packing as in Figures 1 and 2. The pore space is the space between the rods. The entry capillary pressure corresponds to the configuration when the fluid-fluid interface is circular and just touches the solid rods as illustrated in Figure 2. Further drainage of the wetting fluid will reduce the radius of curvature of the fluid interface between the rods and

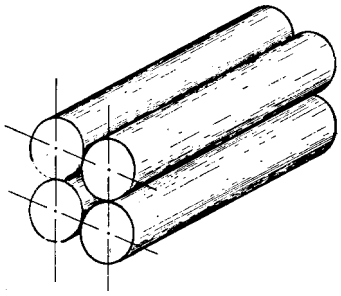

Fig. 1 Cubic packing of circular rods. (Collins 1961)

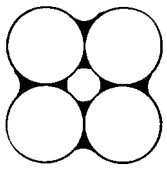

Fig. 2 Liquid -air interfaces in packing of glass rods (Collins, 1961)

thus increase the capillary pressure. The capillary pressure curve can be calculated exactly for this geometry (Collins 1961) and is illustrated in Figure 3. If one calculates the dimensionless entry capillary pressure in this geometry, it will be found to be equal to $2\left(1+\sqrt{2}\right)$ or 4.83. Thus the curve in Figure 3 should be joined by a horizontal line at this value of the dimensionless capillary pressure and the part of the curve below this value is unstable. A bundle of cubic packed rods will jump from a saturation of 1.0 to about 0.05 as the wetting fluid is drained from the bundle.

These examples illustrate the limiting cases of the geometry governing the capillary pressure curve. Real system will have combination of pore size distribution and crevices contributing to the capillary pressure curves. Also, real systems will have trapping and wettability phenomena discussed in Chapter 5 of CENG 571.

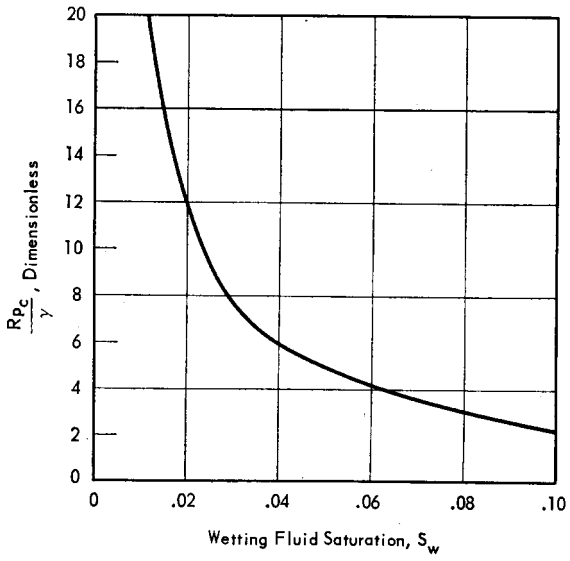

Fig. 3 Computed capillary pressure-wetting fluid saturation relationship for water in cubic packing of glass rods. (Collins, 1961)

Hydrostatic Fluid Distribution

Suppose that water and oil (or air) existed in hydrostatic equilibrium. Let z be the vertical distance measured upward from the free water level. The hydrostatic pressure distribution in the water and oil phases are then given by the following equations.

$$p_w(z) = p_w(z=0) - \rho_w g z$$
$$p_o(z) = p_o(z=0) - \rho_o g z$$

The oil-water capillary pressure is defined as the difference between the oil and water pressures.

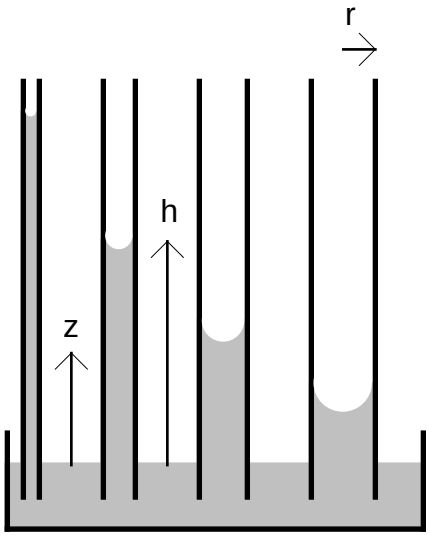

Fig. 4 Capillary rise of wetting phase in capillaries of different radii

$$
\begin{aligned}
P_c(z) &\equiv p_o(z) - p_w(z) \\
&= P_c(z=0) + (\rho_w - \rho_o) g\, z \\
&= (\rho_w - \rho_o) g\, z
\end{aligned}
$$

The capillary pressure at the free water level (*z=0*) is zero because the interface is flat there. In the absence of flat interfaces as in porous media, the free water level is defined as the elevation where the capillary pressure is zero. The above equation gives the mapping between the elevation and the capillary pressure. The capillary pressure is proportional to the elevation above the free water level and the constant of proportionality is the product of the density difference and the acceleration due to gravity.

Recall the Young-Laplace equation for the pressure drop across a curved interface.

$$
\begin{aligned}
\Delta p &= \sigma \left(\frac{1}{r_1} + \frac{1}{r_2} \right) \\
&= P_c
\end{aligned}
$$

The meniscus (interface) in a small circular, water-wet capillary tube is a hemisphere (if the Bond number is small enough) and the two principal radii of curvature are equal to each other and equal to the capillary radius. Thus the elevation, *h*, of the meniscus in a capillary of radius *r* is the elevation where the pressure drop across the meniscus is equal to the capillary pressure given by the hydrostatic pressure distribution.

$$
\begin{aligned}
P_c &= \frac{2\sigma}{r} \\
&= (\rho_w - \rho_o) g\, h
\end{aligned}
$$

This equation expresses the meniscus elevation as a function of the capillary radius. At an elevation *h*, all capillaries with a radius greater than *r(h)* are occupied by oil (or air) and all capillaries with a radius less than *r(h)* are occupied by water. If one is given the cumulative distribution of the pore radii (the capillary pressure curve), then the water saturation as a function of elevation above the free water level can be calculated.

$$
\begin{aligned}
P_c(S_w) &= (\rho_w - \rho_o) g\, h \\
h(S_w) &= \frac{P_c(S_w)}{(\rho_w - \rho_o) g} \\
S_w(h) &= S_w^{-1}\left[P_c = (\rho_w - \rho_o) g\, h \right]
\end{aligned}
$$

One may argue that the bundle of capillary tubes model is not realistic because the water in a small capillary is separated from the oil (or air) in a large capillary by the capillary walls rather than a fluid-fluid interface as in most porous media. Lets consider the case of a bundle of rods illustrated in Figures 1 and 2. Suppose these rods are vertical. The pore space will be completely saturated with water for capillary pressures below the entry capillary pressure. The elevation of unit water saturation above the free water level can be computed as follows.

$$h\left(\text{Max for } S=1.0\right)=\frac{2\sigma}{\left(\sqrt{2}-1\right)R\left(\rho_w-\rho_o\right)g}$$

Above this elevation the water saturation will decrease as illustrated in Figure 3. The saturation profile and pore fluid distribution is illustrated in Figure 5. In this illustration the water and oil (or air) exist together in the same pore (above the entry capillary pressure) and the pressure difference or capillary pressure is reflected in the curvature of the interface separating the phases. Natural porous media is generally not a bundle of capillaries or rods but these two media illustrate the features of the pore geometry of porous media that determine the shape of the capillary pressure curve.

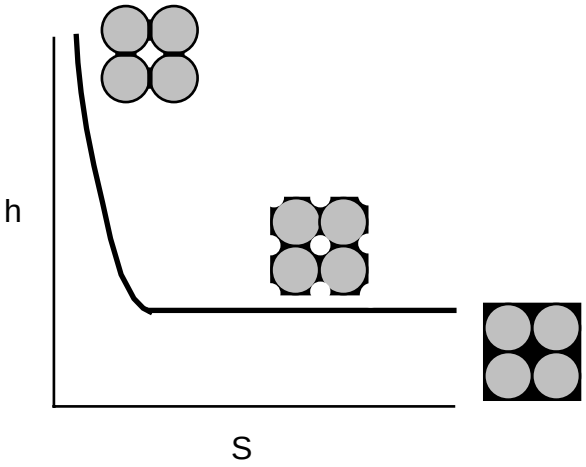

Fig. 5 Capillary desaturation in a vertical bundle of rods of equal radii

Dimensionless Capillary Pressure

We mentioned earlier that mercury-air capillary pressure measurement can be used to characterize the pore size distribution. However, it is not appropriate to directly use a mercury-air capillary pressure curve to determine the hydrostatic distribution of oil and water because the mercury-air surface tension is about an order of magnitude greater than the oil-water interfacial tension. Is there some way we can compensate for the difference of the interfacial tensions?

If one were to view a micro-photograph of a bead pack made of 10 mm or 10 μm beads, one would not know which was which without a scale on the photographs, i.e. they are geometrically similar. Also one would expect that geometrically similar packs should have capillary pressure curves that have something in similar.

Capillary pressure is a measure of the curvature of the interface separating the two phases and a given pore fraction occupied by each phase. Curvature is a geometric quantity having the units of reciprocal length. We should be able to determine a characteristic length of the porous media (e.g. effective pore radius) to make the curvature dimensionless. Would this be adequate to make dimensionless capillary pressure curves similar? No. When we described the pore size distribution with the log normal distribution the distribution was described by the log mean radius and standard deviation. The shape of the capillary pressure should also be a function of the normalized standard deviation. Porous media that have a log normal pore size distribution and the same normalized standard deviation are geometrically similar. Rocks that have micro porosity (clays, chert) or vugs do not have a log normal pore size distribution and a more complex model will be needed. Geometrically similar pore size distribution is a necessary but not sufficient condition for the dimensionless capillary pressure to be similar. It is the interfacial curvature that determines the capillary pressure and the interfacial curvature is dependent on the contact angles that the fluid interfaces makes with the pore walls. Thus identical wettability is another condition for similar dimensionless capillary pressure curves. Some people have attempted to compensate for different wettability by multiplying the interfacial tension by the cosine of the contact angle. This will work only in cylindrical capillaries.

To see how to make the capillary pressure dimensionless, consider the case of a circular capillary tube.

$$S_w = 1, \quad P_c < \frac{2\sigma}{r}$$

$$S_w = 0, \quad P_c > \frac{2\sigma}{r}$$

This can be made dimensionless as follows.

$$S_w = 1, \quad \frac{r}{\sigma} P_c = P_{cD}^* < 2$$

$$S_w = 0, \quad \frac{r}{\sigma} P_c = P_{cD}^* > 2$$

Recall CENG 571, Chapter 3, Rock Properties, Permeability, Packed Bed of Spherical Particles. The equivalent capillary radius of a packed bed of spherical particles was expressed in terms of the permeability and porosity.

$$r_{eq} = \sqrt{\frac{50k}{3\phi}}$$

If we substitute this expression for the equivalent radius into the previous equation, we then can express the dimensionless capillary pressure in terms of measurable properties. The numerical factor will not be included in the definition of the dimensionless capillary pressure. The dimensionless capillary pressure for a single capillary is then as follows.

$$S_w = 1, \quad \frac{\sqrt{\frac{k}{\phi}}}{\sigma} P_c = P_{cD} < 2\sqrt{\frac{3}{50}} = 0.49$$

$$S_w = 0, \quad \frac{\sqrt{\frac{k}{\phi}}}{\sigma} P_c = P_{cD} > 2\sqrt{\frac{3}{50}} = 0.49$$

The proceeding discussion was for a porous medium consisting of a bundle of identical capillary tubes. In this case the saturation jumps from 1 to 0 as the dimensionless capillary pressure exceeds 0.49. Natural porous media have a distribution of pore sizes and have crevice like spaces between particles similar to the bundle of rods. Thus natural porous media have the saturation change over a range of capillary pressures rather than at a single value. The dimensionless capillary pressure then is a function of saturation. This function is traditionally called the Leverett ***j*** function. We will use the upper case ***J*** in keeping with the SPE nomenclature of using the upper case for P_C. Figure 6 illustrates a correlation of sand pack capillary pressures by Leverett using this function. This functions correlated data over several orders of magnitude change in permeability. Also, notice that the J function value where most of the saturation change occurs is close to the value of 0.49 for a bundle of identical capillary tubes. (The square root sign is missing in Figure 6.) Notice that the wetting phase saturation appears to asymptote at about 0.08. This is because with beads or sand grains, unlike the pack of rods, the fluid in the pendular spaces are disconnected except for a thin film on the solid surfaces. Drainage is very slow through these thin films and due to the limited patience of the person making the measurement, the saturation is called the "irreducible saturation", e.g., S_{wir}.

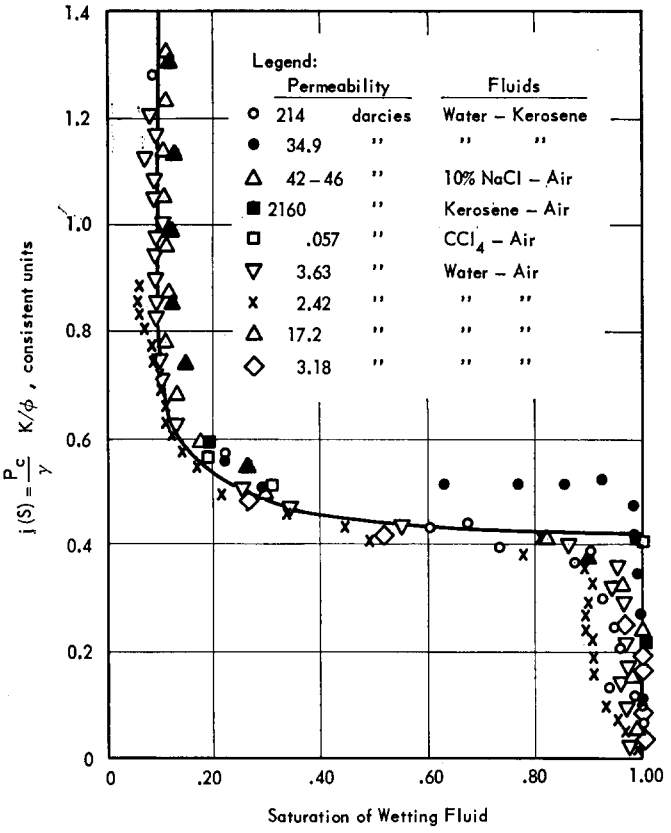

Fig. 6 The Leverett J(S) function for unconsolidated sands [Collins, 1961 (Leverett, 1941)].

Figures 3.7 and 3.8 illustrate the Leverett J functions for Berea sandstone and Indiana limestone. The Berea data were fit with a Thomeer model and the limestone data were fit with a lognormal model. It is significant to notice the much larger range of J function over which the saturation continues to change compared to the sand packs. This reflects a much larger distribution of pore sizes compared to the sand packs. The Berea sandstone contains clays in addition to having a distribution of sand grain sizes. The different shapes of the J(S) function show that Berea sandstone and Indiana limestone are not geometrically similar. The J(S) function of geometrically similar rocks will overlay for samples that may differ in permeability by an order of magnitude. Thus the Leverett J(S) function should be used to average data from several samples and to look for outliers or different rock types.

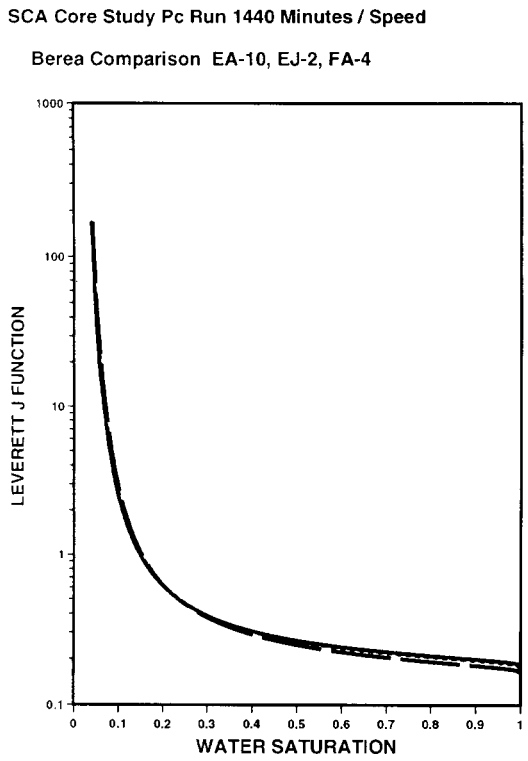

Fig. 7 Leverett J function of three Berea sandstone samples, k=763±11 md, ϕ=0.230±0.001.

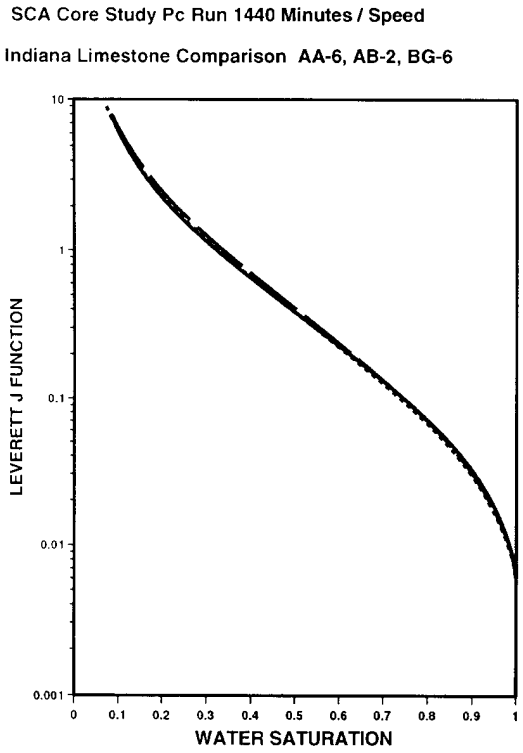

Fig. 8 Leverett J function of three Indiana limestone samples, k=1.1±0.2 md, ϕ=0.125±0.005.

Calculation of Hydrostatic Saturation Profile

If the Leverett J function is known for each rock type and the profile of rock type, permeability, and porosity are known in addition to the depth of the free water level, the saturation profile can be calculated. Figure 3.9 illustrates the saturation profile calculated for an actual reservoir by using a single J(S) curve.

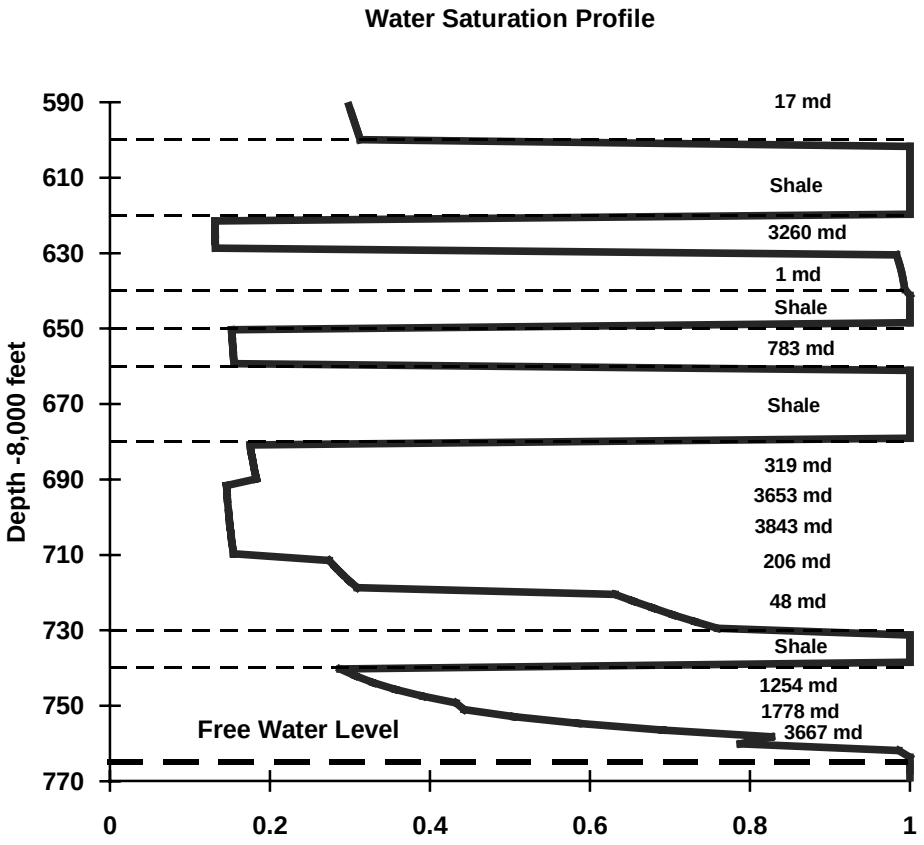

Fig. 3.9 Water saturation profile calculated from Leverett J(S) function and permeability and porosity profile.

Profile of Water, Oil, and Gas

The hydrostatic profile of water, oil, and gas can be calculated if the Leverett J function is known and it can be assumed that the liquid-gas J function has the same shape as the water-wet J function since the liquid phase is usually wetting compared to the gas phase. A free liquid level needs to be specified. The following assumptions are made. (1) Where the oil phase exists, the water saturation is determined by the usual water-oil hydrostatic relations. (2) Where the oil phase exists, the liquid-gas saturation profile is determined by the density difference and interfacial tension between oil and gas. (3) Where the oil

saturation is zero, the water saturation profile is determined by the density difference between water and gas and the interfacial tension is the lesser of the water-gas interfacial tension and the sum of the water-oil and oil-gas interfacial tensions. If the water-gas tension is greater than the sum of the above mentioned tensions, the oil will spontaneously spread as a thin film between the water and gas. The actual tension will be between these two limiting values.

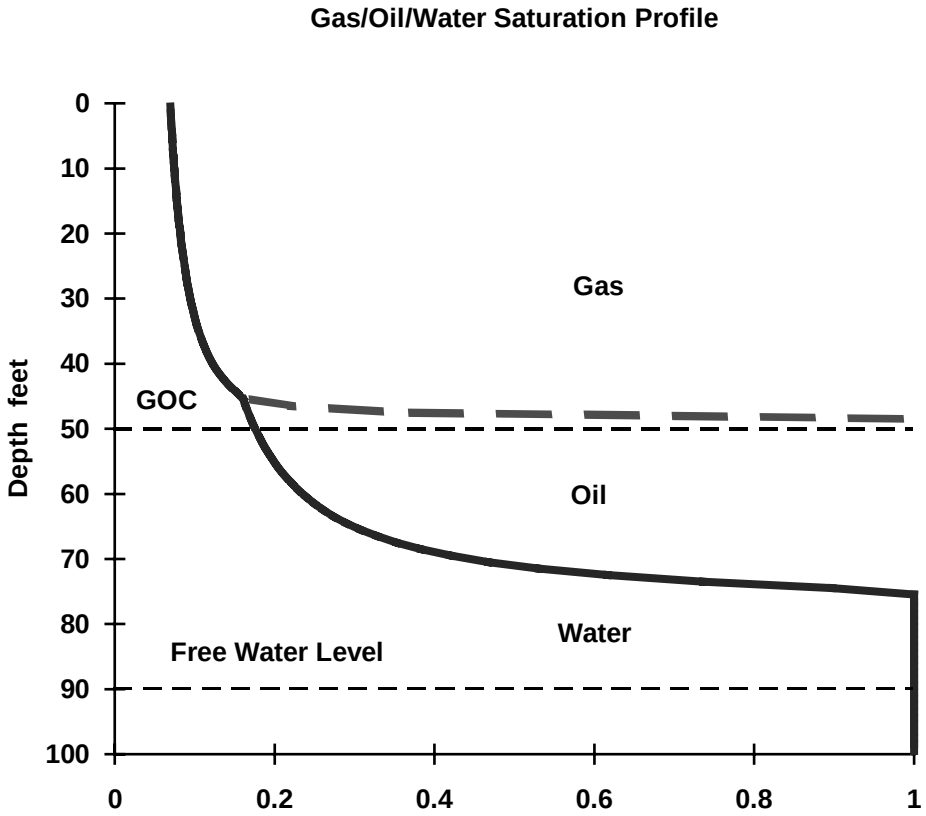

Fig. 3.10 Saturation profile for water, oil, and gas phases

Reservoir Seals

You may have wondered about what causes oil to stop migrating upward by buoyancy and accumulate in a geological "trap". The saturation profile in Figure 3.9 should give a clue. Recall that generally oil is the nonwetting phase and the capillary entry pressure must be exceeded before a nonwetting phase will enter a porous medium that is saturated with the wetting phase. We saw from the discussion on dimensionless capillary pressure that the capillary entry pressure is inversely proportional to the square root of the permeability. We can see in Figure 3.9 that oil just entered a 1 md sand that is 120 feet above the free water level. A shale may be orders of magnitude lower in permeability and thus act as an effective seal. However, if the shale is oil-wet, the oil will slowly leak through the shale and can escape from a trap if given a geological time scale.

Outflow Boundary Condition

When the capillary pressure is neglected as in the Buckley-Leverett problem, the only boundary condition is the inflow boundary condition. With capillary pressure, the mass conservation is second order in the spatial derivatives and a boundary condition is needed for the outflow end of finite systems. The usual boundary condition for the outflow end is either no flow of the wetting phase or zero capillary pressure. Suppose a water-wet rock sample that is saturated with oil at a low water saturation is water flooded. Initially, no water can flow back in to the sample from the outflow end piece (e.g. perforated plate) because it is filled with oil that is flowing out from the core, i.e. there is no water. Suppose that the water relative permeability at the outflow end is not zero and some water starts to flow out. If the outflow end is freely suspended, the water seeping out of the rock is a connected phase since it wets the rock and it will gather into a drop that is suspended from the outflow end of the rock. The curvature of this drop will be small compared to the curvature of the interfaces in the pore spaces and we can assume that the curvature is zero, i.e. assume zero capillary pressure. If the water saturation at the outflow end is low, then the capillary pressure will be high and there will be a discontinuity or a large gradient in the capillary pressure at the outflow end. If the magnitude of the gradient in the capillary pressure is greater than the magnitude of the oil pressure gradient, then the gradient in the water pressure will be such that the water will flow back into the rock.

$$\nabla p_w = \nabla p_o - \nabla P_c$$

Thus water can not flow out of the rock until the capillary pressure gradient becomes less than the oil pressure gradient. As more water accumulates near the outflow end, the water saturation increases, the capillary pressure decreases, and finally when the capillary pressure gradient becomes less than the oil pressure gradient, the water will flow out of the rock. This capillary end effect may result in a higher water saturation at the outflow end compared to the saturation ahead of the displacement front. This high water saturation at the outflow end may result in a reduction of the oil relative permeability that is not taken into account with the Buckley-Leverett theory.

If the wetting phase is displaced by the nonwetting phase, then the wetting phase will produce from the beginning but will cease to flow when the capillary pressure gradient becomes equal to the nonwetting phase pressure gradient. This is the principle for making capillary pressure measurements with the centrifuge method (O' Meara, Hirasaki, Rohan, 1992). However, in flow displacement experiments, the termination of production has often led the experimentalist to the mistaken belief that the system is at the residual saturation where the relative permeability is zero.

Counter-current Imbibition

So far we have only discussed cases where one end is the inflow end and the other end is the outflow end. With capillary pressure, one end can have both inflow of the wetting phase and outflow of the nonwetting phase. If the other end is closed or the system extends to infinity, the flow will be counter-current with the total flux equal to zero. Counter current imbibition is an important displacement process in heterogeneous systems. e.g., Water will tend to channel through fractures but counter-current imbibition can imbibe water into the matrix and thus displace the oil.

Methods of Measurement

Mercury Injection The mercury injection apparatus is illustrated in Figure 3.11. The sample is placed in a chamber and is evacuated. Mercury in introduced at a number of pressure increments and the cumulative volume of mercury injected is measured. This procedure is called pressure controlled porosimetry. Another procedure introduces mercury at a constant volumetric rate and the pressure response is measured with high resolution. This procedure, called volumetric controlled porosimetry gives much more information about the pore structure.

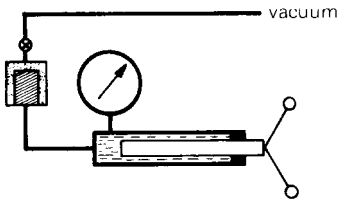

Fig. 3.11 Mercury injection (Marle, 1981)

Centrifuge Displacement Figure 3.12 illustrates the centrifuge displacement apparatus (O'Meara, Hirasaki, Rohan, 1992). The rock sample in this illustration is surrounded by the less dense phase and the more dense phase is collected in the collection vial where the volume is measured by strobe illumination and a linear video camera. If the less dense fluid is to be the displaced phase, the sample is surrounded by the more dense phase and the displaced phase is collected in a collection vial that is placed opposite side of the sample. The measurements are made at a number of speed steps and the cumulative volume of production is recorded. From material balance, the production gives the average saturation in the sample. The hydrostatic saturation profile at each speed can be calculated at each speed by assuming that the free water (wetting phase) level or zero capillary pressure is at the outflow end of the sample and if given a model of the capillary pressure curve. The average saturation can be calculated from the saturation profile. This average saturation is expressed as a function of the capillary pressure at the inflow end of the sample. The parameters of the capillary pressure model can be estimated from a best fit of the calculated average saturation versus

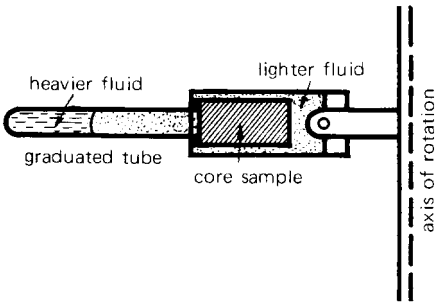

Fig. 3.12 Centrifuge displacement (Marle, 1981)

speed with the measured values. Figs. 3.13 and 3.14 illustrates the fit of the measured average saturations (symbols) and the calculated capillary pressure curve for a Berea sandstone sample.

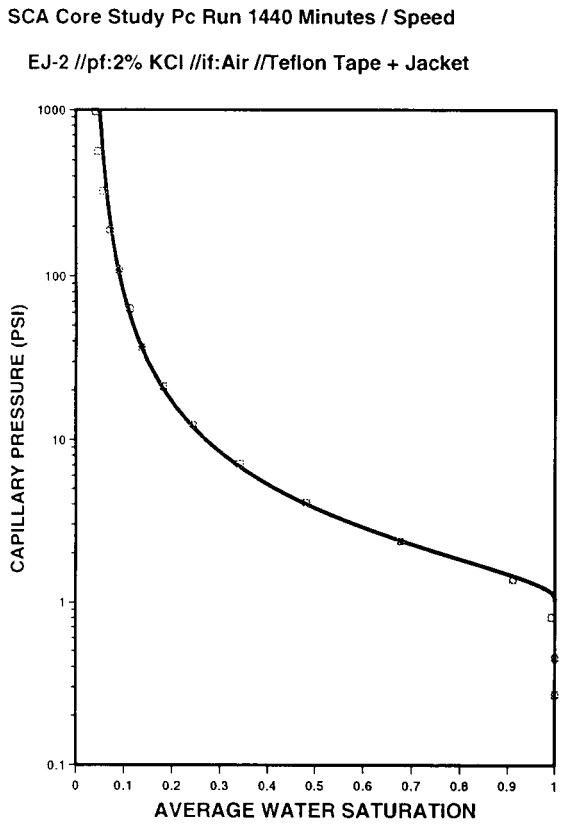

Fig. 3.13 Measured average saturation and best fit of data

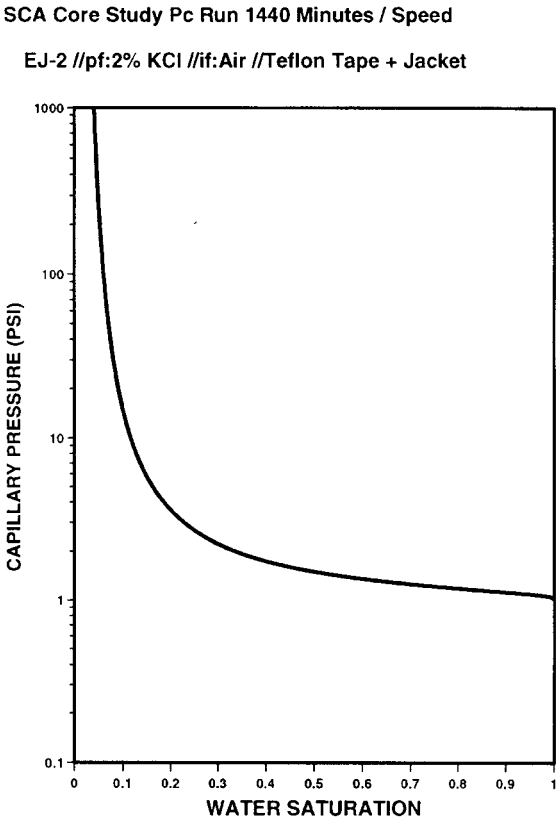

Fig. 3.14 Capillary pressure curve that resulted is best fit of average saturation measurements. Thomeer model

Capillary Diaphragm

Fig. 3.15 illustrates measurement of capillary pressure by the capillary diaphragm and porous plate methods. A diaphragm allows only the fluid that wets the diaphragm to exit the sample chamber. If capillary contact is maintained, the fluid that wets the diaphragm is at one atmosphere at equilibrium and the pressure of the other fluid is controlled. The fluid exiting the sample through the diaphragm is recorded and the average saturation determined by material balance.

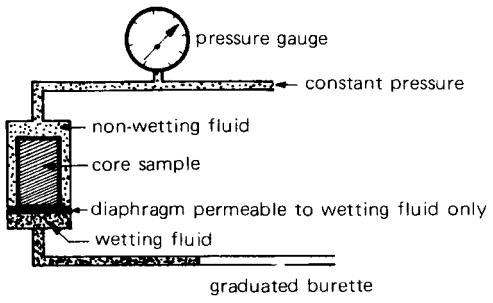

Fig. 3.15 Capillary diaphragm apparatus (Marle, 1981)

Capillary Pressure Models

Capillary pressure data directly from the laboratory is subject to "noise" in the measurements due to small, unavoidable errors. This noise becomes an even worse problem in numerical simulations because the derivative of the capillary pressure curve is needed for semi-implicit methods. Thus some means is needed to "filter" the noise from the experimental data. One approach is to fit the data to a model that is appropriate for the rock type under study. The models are used to fit measured data and summarize the data with a small set of parameters. The repetitive evaluation of the models may be too costly to be used in large scale reservoir simulations. The models may be used to generate tabulated data for input to the simulator and have the simulator do a table look-up with a spline function that gives continuous slopes.

The following models are not unique but have been adequate for most systems encountered. The Thomeer models is good for sandstones without micro porosity. The lognormal model is good for unimodal carbonates. The bimodal lognormal models are needed to represent sandstones with micro porosity (e.g., chlorite coated sand grains) and vuggy carbonates. The bimodal models will not be given here.

The following models describe the dimensionless capillary pressure function or the Leverett J function. The definition of the J function gives the dependence of the capillary pressure on the interfacial tension and the ratio of permeability and porosity. In the following, it is assumed that water is the wetting phase.

Thomeer Model

$$\frac{S_w - S_{wr}}{S_{wi} - S_{wr}} = \begin{cases} 1.0, & J < J_e = C_1 \\ 1.0 - \exp\left\{ \dfrac{C_2}{\ln\left[\dfrac{C_1}{J} \right]} \right\}, & J > J_e = C_1 \end{cases}$$

The initial water saturation, S_{wi}, is a specified quantity. The residual water saturation, S_{wr}, is defined here as the asymptotic saturation where the capillary pressure approaches infinity. C_1 is the entry value of the Leverett J function. C_2 is 2.303 times the pore geometric factor. The latter three parameters are estimated by fitting the measured data.

Estimated Thomeer Parameters for Figures 3.13 and 3.14

Parameter	Estimated value	Standard deviation
S_{wr}	0.00	0.01
C_1	0.17	0.01
C_2	0.29	0.04

Log Normal Model

$$\frac{S_w - S_{wr}}{S_{wi} - S_{wr}} = \begin{cases} 1.0, & J < J_e = C_1 \\ \dfrac{1}{2}\operatorname{erfc}\left\{ \dfrac{\ln\left[\dfrac{(J - C_1)}{C_2} \right]}{C_3} \right\}, & J > J_e = C_1 \end{cases}$$

The parameters that are different from the Thomeer model are C_2 which is the median value of the J function minus C_1 and C_3 is a measure of the width of the distribution of the logarithm of the Leverett J function.

Estimated Log Normal Parameters for Figure 3.8

Parameter	Estimated value	Standard deviation
S_{wr}	0.02	0.05
C_1	0.006	0.007
C_2	0.36	0.05
C_3	2.9	0.3

Effect of Wettability

So far we have considered systems which are water-wet. Systems with crude oil can have much more complex wetting conditions. Figure 3.16 shows a series of secondary drainage and imbibition measurements for wettability evaluation. The "as received" condition cores were wrapped and refrigerated for two years. Different cleaning methods were used and the wettability evaluated by making measurements with refined oil. The drainage curve for the "as received" condition is vertical, indicating that water is trapped as a discontinuous phase. After cleaning, the drainage curves are more curved and go to lower water saturations. This is what one would expect for water-wet conditions.

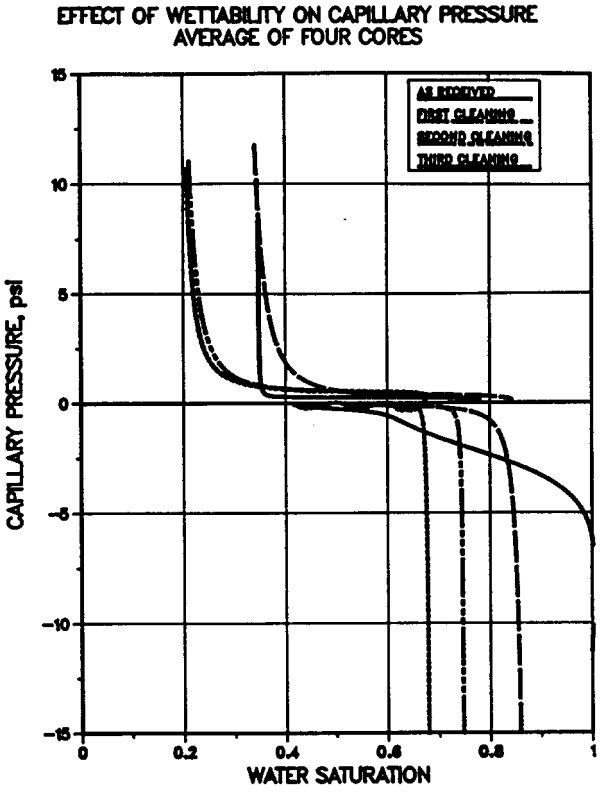

Fig. 3.16 Secondary drainage and imbibition measurements for wettability evaluation (Hirasaki, Rohan, Dubey, Niko, 1990)

The imbibition curves for the "as received" condition is curved and goes to zero oil saturation. This is an indication of film drainage where the oil remains connected and goes to a low residual oil saturation. With each step of cleaning, the imbibition curves become more vertical and have a larger residual oil saturation. This is an indication that oil is trapped as a discontinuous phase.

References

Collins, R.E., Flow of Fluids through Porous Materials, Reinhold Publishing Corp., New York, 1961.

Hirasaki, G.J., Rohan, J.A., Dubey, S.T., and Niko, H., "Wettability Evaluation during Restored-State Core Analysis", SPE 20506, paper presented at the 65th Annual Technical Conference of SPE, New Orleans, September 23-26, 1990.

Leverett, M.C., Trans. AIME, Vol 195, (1950), 275.

Marle, C.M., Multiphase Flow in Porous Media, Gulf Publishing Co., Houston, 1981.

O'Meara, D.J., Jr., Hirasaki, G.J., and Rohan, J.A.: "Centrifuge Measurement of Capillary Pressure: Part 1 - Outflow Boundary Condition", SPE Reservoir Engineering, February 1992, 133-142.